Science Robotics

robotics.sciencemag.org/cgi/content/full/2/9/eaan6357/DC1

Supplementary Materials for

New soft robots really suck: Vacuum-powered systems empower diverse capabilities

Matthew A. Robertson and Jamie Paik*

*Corresponding author. Email: jamie.paik@epfl.ch

Published 30 August 2017, *Sci. Robot.* **2**, eaan6357 (2017)
DOI: 10.1126/scirobotics.aan6357

The PDF file includes:

Other Supplementary Material for this manuscript includes the following:
(available at robotics.sciencemag.org/cgi/content/full/2/9/eaan6357/DC1)

Movie S1 (.mp4 format). Binary control of 3-DoF V-SPA array without modular interface.
Movie S2 (.mp4 format). Binary workspace of V-SPA Module.
Movie S3 (.mp4 format). Continuum robot repeatability test.
Movie S4 (.mp4 format). Vacuum suction manipulation with continuum robot.
Movie S5 (.mp4 format). Vacuum suction climbing with payload.
Movie S6 (.mp4 format). Vacuum robot locomotion.

Supplementary Materials

Figures

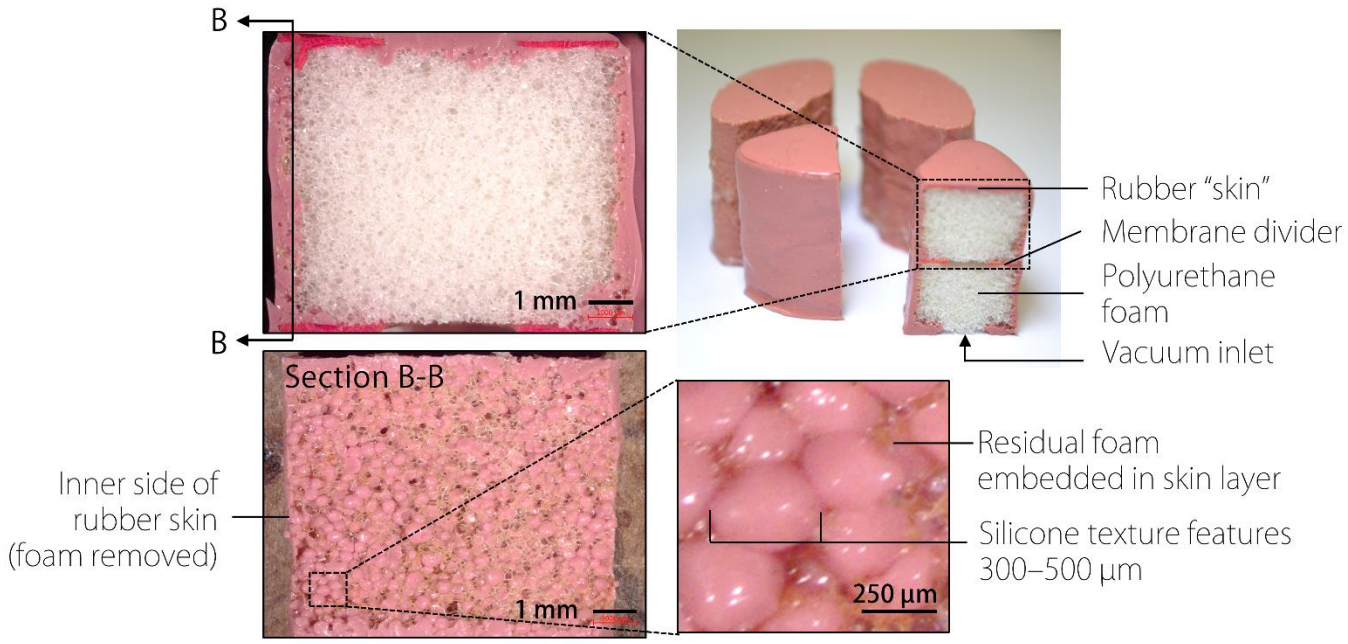

Fig. S1. Anatomy of a V-SPA. When uncured silicone is applied to the surface of the foam core it penetrates to a depth limited by its viscosity and liquid surface tension, and then remains primarily on the surface of the foam. The bubble-like texture features visible in the cross section are formed across the open pores of the foam core, while some foam remains embedded in the skin layer of the actuator. It can be seen that the wall thickness for V-SPAs is very non-uniform, however this does not significantly impede repeatability or robustness as the actuators perform well, with minimal variability, in testing over many cycles.

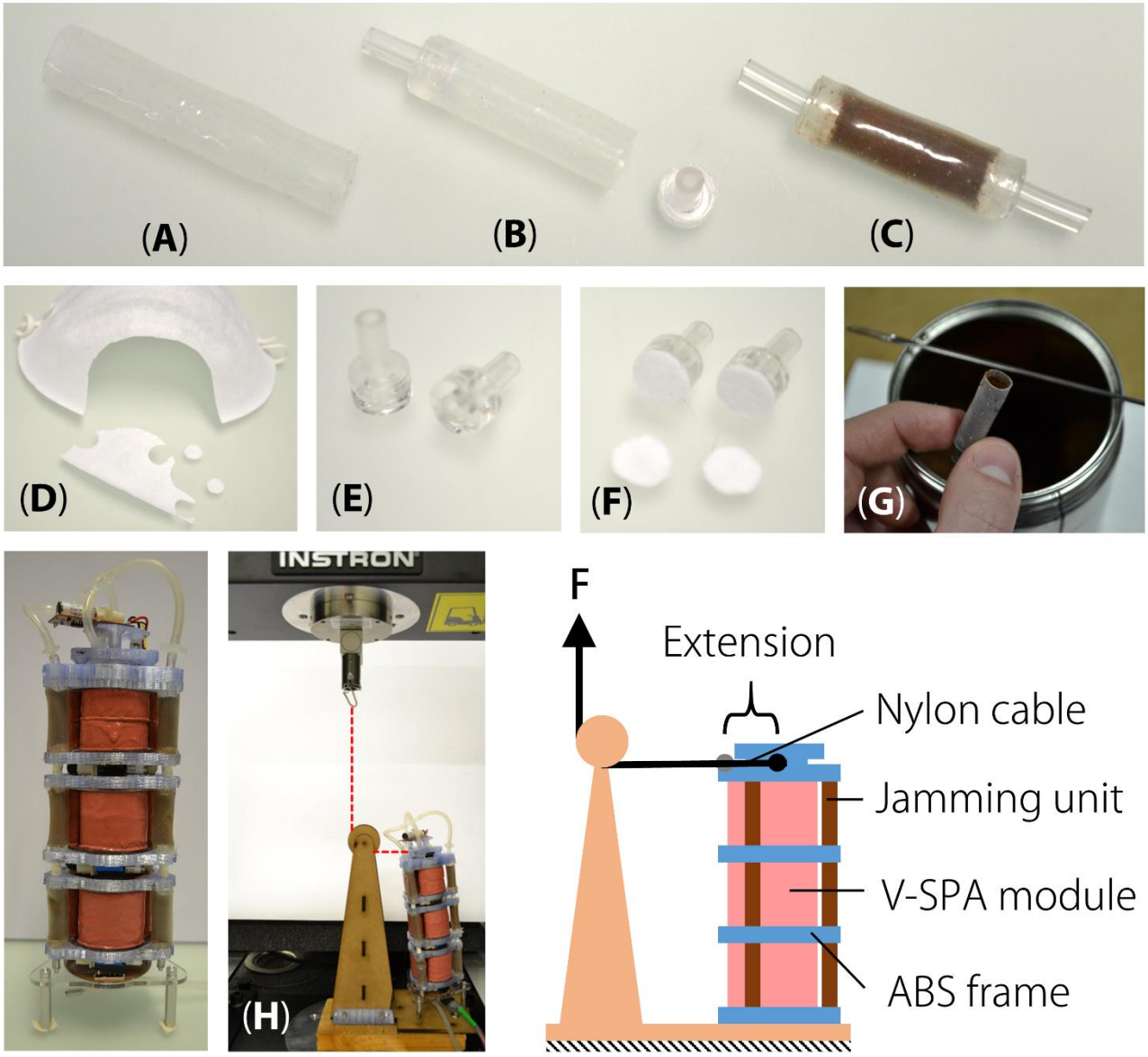

Fig. S2. Fabrication and testing of jamming module. Jamming units are fabricated by first creating thin walled silicone tubes using Dragon Skin-50 brushed onto a cylindrical form. The resulting cured silicone tube is peeled off the form and a segment is cut to make one jamming unit (**A**). End caps are attached to each end of the tube (**B**), after being filled with fine ground coffee particles (**C**). To ensure the coffee is not drawn out of the module from the vacuum supply, disc shaped filters are cut from a paper dust mask (**D**). Before inserting into the silicone tube, the end caps are fitted with segments of vinyl tubing to attach to the vacuum supply (**E**) and the paper filters are glued on the inside surface (**F**). Filling with coffee is accomplished by first gluing one end cap in place to the silicone tube segment, scooping and packing in a measured amount of coffee to the open end, and then finally gluing the other end cap in place (**G**). Photo (**H**) depicts the actual test set up used to measure the stiffness of the stacked modules and jamming units with a dashed red line superimposed over the translucent nylon cable. The adjacent illustration shows the setup with an explanation of important components, as well as the parameters measured during the stiffness evaluation.

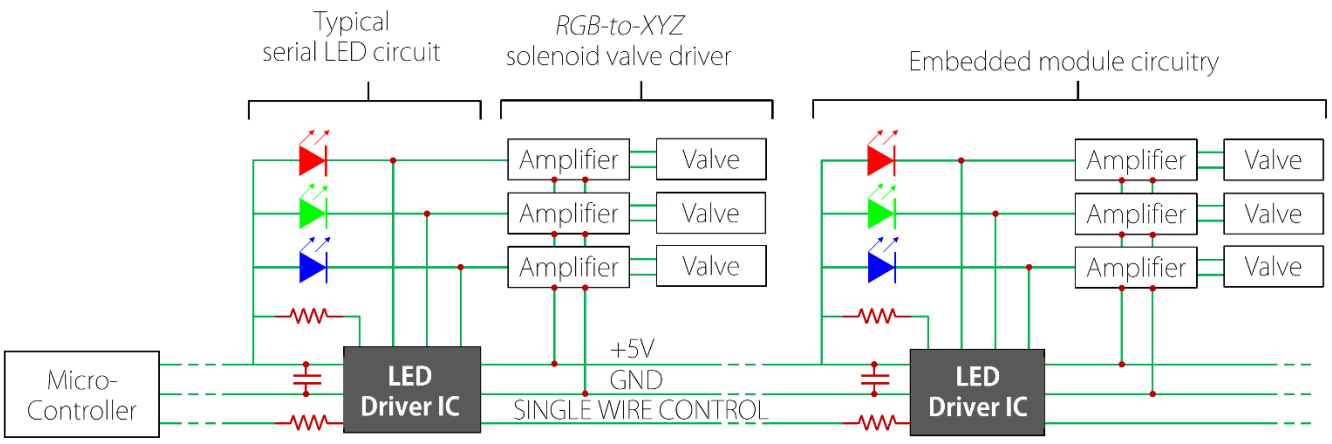

Fig. S3. Single wire module networking with serial LED driver IC. Circuitry embedded within each actuator module contains a three-channel IC designed and widely used for controlling multi-color Red-Green-Blue (RGB) LEDs. In parallel with the color channels, these chips can be leveraged to provide three-channel control of solenoid valves through an amplifier. Each channel is addressed over a single wire interface, using a time-based data packet structure which is passed to subsequent drivers connected in series. Communication libraries for Arduino based microcontrollers are available from Adafruit Industries on GitHub (*51*).

Movie Captions

Movie S1. Binary control of 3-DoF V-SPA array without modular interface. A circular array of V-SPAs are assembled on a distribution manifold with each actuator connected to a vacuum supply through a manually triggered solenoid valve. The actuators are first activated alone to illustrate the nominal mode of vacuum-induced buckling. The addition of a plate to the top surface of all actuators with Loctite 406 adhesive prevents buckling of the actuator top surface and the added constraint of stiffness from the other unactuated V-SPAs yields an angular deflection of the upper plate. In addition to singular, binary activation of the V-SPAs, they are also activated in pairs to yield a total of 6 possible discrete angular positions of the upper plate, spaced at 60° around the center of the array.

Movie S2. Binary workspace of V-SPA Module. A 3-DoF V-SPA Module demonstrates rapid angular deflection as shown in randomized directions. Discrete, binary control is utilized to operate each V-SPA individually to produce motion in three primary directions at 120° spacing around the central axis of the actuator. While not shown here, finer, more continuous control of the direction of deflection or magnitude of the angle is possible with this module utilizing PWM vacuum pressure control.

Movie S3. Continuum robot repeatability test. A ten-cycle test was performed under an OptiTrack motion capture system, which accurately recorded the trajectory of the continuum robot mounted vertically. The repeatability of the robot was evaluated by analyzing the path of the robot endpoint, which in the video is shown to be a single, offset reflective marker. While the data set for the test shown in this video was not recorded properly, another test was conducted to produce the data shown in **Figure 4**, for which three markers were used to track the calculated center point of the distal module. Black tape was used to obscure other reflective components on the robot which interfere with the motion tracking system. The activation pattern that can be seen was selected deliberately as a progression from the most distal module to that most proximal to the base with a delay between each activation to limit the magnitude of oscillation caused by the actuator deflection, and not a direct consequence of the inflation or manifold dynamics. All actuators on a side can in fact be activated simultaneously, but the resulting torque from the sudden strong movement would result in longer waiting between subsequent cycles to allow dissipation of large oscillations.

Movie S4. Vacuum suction manipulation with continuum robot. A single active suction cup module is added to the distal end of a Vacuum-powered Continuum Robot comprised of three V-SPA Modules to serve as an end effector. A valve connected to the internal volume of the suction cup connects it to the central vacuum supply to enable selective adhesion or release of smooth, flat objects. The robot demonstrates a simple pick-and-place operation by moving empty acrylic containers from a gravity-fed supply rack to target bins on either side of the robot base. The motion of the robot is programmed open-loop and the adhesion of the particular suction cup used depends is sensitive to alignment, but could easily be replaced with a more compliant, auto-aligning variety designed more specifically for such operations. The suction cup used was adapted from a fixture system designed for long-term adhesion to smooth bathroom tiles.

Movie S5. Vacuum suction climbing with payload. The payload capacity of a climbing robot was estimated using increments of 10 g mass weights suspended from a nylon cable. The largest mass tolerated that did not inhibit vertical progress in climbing was found to be 70 g. The next tested increment of 80 g was found to disrupt the climbing pattern of the robot, however this may result from the given controller used for the vertical gait and as a consequence of additional passive degrees of freedom at the lower “foot” which allows the robot to briefly fall away from the wall. Beyond this

threshold, better timing (faster release of footholds and body actuation) may be used to prevent falling, although previous tests also found that this would likely yield slower climbing speeds.

Movie S6. Vacuum robot locomotion. Three gaits are demonstrated, in four configurations; a vertical climbing gait, with two actuator modules, and two additional suction cup modules achieves locomotion at 2 mm/s, or 0.01 Body Lengths per second (BL/s). A rolling gait and wave gait pattern are demonstrated with a 5 module, 15 DoF continuum robot, while the wave gait is repeated with a 3 module, 9 DoF robot. The shorter 3 module continuum robot achieves faster forward locomotion of 11 mm/s, than the 5 module version of 5 mm/s, while the rolling gait achieves the fastest average speed at 60 mm/s. None of the gaits tested were optimized for speed, but the variety is shown to illustrate the characteristic diversity of the different locomotion modes. The robots shown are powered from dual pneumatic ports at each end of the body to compensate for pressure and flow drop in undersized module ports, although both supplies are connected to a single, internal central supply line connected to every V-SPA in the robot through localized solenoid valves.